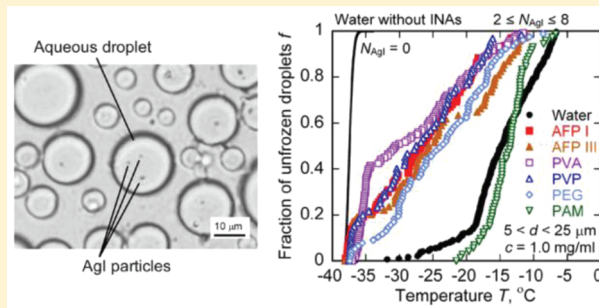


# Inactivation of Ice Nucleating Activity of Silver Iodide by Antifreeze Proteins and Synthetic Polymers

Takaaki Inada,\*<sup>†</sup> Toshie Koyama,<sup>†</sup> Fumitoshi Goto,<sup>‡</sup> and Takafumi Seto<sup>‡</sup><sup>†</sup>National Institute of Advanced Industrial Science and Technology (AIST), Namiki 1-2-1, Tsukuba, Ibaraki 305-8564, Japan<sup>‡</sup>Graduate School of Natural Science and Technology, Kanazawa University, Kakuma, Kanazawa 920-1192, Japan

## S Supporting Information

**ABSTRACT:** Antifreeze proteins (AFPs) and poly(vinyl alcohol) (PVA) are known as anti-ice nucleating agents (anti-INAs), which inhibit ice nucleation initiated by ice nucleating agents (INAs). Although the effectiveness of anti-INAs depends on the type of INA, most previous studies on anti-INAs used only a few types of biological INAs as targets to inactivate. In this study, the effects of fish AFPs (AFP I and AFP III) and PVA on the ice nucleating activity of silver iodide (AgI) were measured by using emulsified solutions. Results showed that AgI was inactivated not only by AFPs and PVA but also by two other polymers previously not considered as anti-INAs, namely, poly(vinylpyrrolidone) and poly(ethylene glycol). Even in the presence of AgI, a non-negligible fraction, typically more than 10%, of emulsified droplets of these anti-INA solutions at 1.0 mg mL<sup>-1</sup> was supercooled to about -37 °C, which corresponds to ice nucleation temperature measured in the absence of AgI.



## 1. INTRODUCTION

Ice nucleation temperature in water droplets can be reduced to about -40 °C by removing ice nucleating agents (INAs) from water, when the droplet diameter is small, on the order of micrometers.<sup>1</sup> In nature, however, various air-borne INAs, from both biological and nonbiological origins, are inevitably present.<sup>2</sup> Therefore, because removing INAs from water becomes difficult as the droplet diameter increases, heterogeneous ice nucleation, which is catalyzed by INAs, is generally observed at temperatures higher than -40 °C.

In freeze-avoiding organisms that survive extremely low temperatures by supercooling without freezing, heterogeneous ice nucleation initiated by INAs present in their body is a fatal problem.<sup>3</sup> To inactivate the INAs, some freeze-avoiding organisms, such as plants, insects, and fish, produce water-soluble anti-ice nucleating agents (anti-INAs) that inhibit heterogeneous ice nucleation in water or aqueous solutions. Most anti-INAs are of biological origin, such as antifreeze proteins (AFPs),<sup>4–13</sup> antifreeze glycoproteins (AFGPs),<sup>7,14,15</sup> a certain protein produced by bacteria,<sup>16</sup> phenylpropanoids,<sup>17</sup> cyclic terpenes,<sup>18</sup> polysaccharides,<sup>19</sup> and flavonol glycosides.<sup>20–22</sup> In addition, several synthetic polymers, such as poly(vinyl alcohol) (PVA),<sup>7,23–27</sup> polyglycerol,<sup>24</sup> and a few copolymers,<sup>28,29</sup> have been reported as potent anti-INAs, and several alkylbenzylidimethylammonium salts have been used as anti-INAs to protect plants from frost injury.<sup>30</sup>

Hypotheses have been proposed to explain the function of anti-INAs. Currently, the most widely accepted hypothesis is that anti-INA molecules mask the ice nucleating sites of INA surfaces and thus prevent ice nucleation initiated at the INA

surfaces by hindering interaction between water molecules and the INAs.<sup>7–11,13–15,24</sup> According to this hypothesis, the effectiveness of anti-INA depends on the type of INA, as suggested by some experimental studies,<sup>7,19,22,24</sup> and therefore, interactions among various combinations of anti-INAs and INAs need to be investigated more systematically to elucidate the function of anti-INAs.<sup>22</sup> Especially for AF(G)Ps and PVA, because depending on the type of INA, both anti-ice nucleating activity and inverse ice nucleating activity have been reported,<sup>7,13</sup> interactions of AF(G)P and PVA molecules with various types of INA need to be further investigated. In most previous studies on anti-INAs, however, only biological INAs such as ice nucleating proteins were used as targets to inactivate.

Another hypothesis to explain the function of anti-INAs is that anti-INA molecules inhibit ice nucleation by directly affecting ice-like water clusters formed on INA surfaces during the nucleation process,<sup>7,8,10,11,13,15,24</sup> although there has been controversy over this hypothesis. Based on experiments and analyses of ice nucleation kinetics, AFP III, which is a fish AFP, reportedly inhibits ice nucleation by the interaction of AFP molecules not only with INA surfaces but also with water clusters on INA surfaces.<sup>8,10,11</sup> However, considering the low diffusion rates of AF(G)P molecules in water, interaction between AF(G)P molecules and water clusters during the nucleation process would seem to be difficult.<sup>15</sup> Emulsified

Received: January 16, 2012

Revised: March 11, 2012

Published: April 16, 2012

droplets have been used to measure the ice nucleation rate in AF(G)P solutions, so as to isolate INAs suspended in the solutions to only a small fraction of the droplets, thus minimizing the effect of INAs on ice nucleation. One report showed that AFGP significantly affects the nucleation rate,<sup>31</sup> suggesting that AFGP molecules might affect water clusters. On the contrary, we recently showed that AFP III has no influence on the nucleation rate, indicating that AFP III does not directly affect water clusters.<sup>32</sup>

Among various anti-INAs, AF(G)Ps have been extensively studied for several decades due to another of their antifreeze activities, namely, inhibition of ice growth in aqueous solutions at temperatures even below the equilibrium melting temperature.<sup>33–36</sup> This growth inhibition is often evaluated based on thermal hysteresis, which is defined as the difference between the nonequilibrium freezing temperature at which ice crystals start to grow and the equilibrium melting temperature. A synthetic polymer, PVA, also exhibits thermal hysteresis activity, although small (about 0.04 °C at 50 mg mL<sup>-1</sup>) compared with those of AF(G)Ps.<sup>37</sup> Therefore, the question remains if the function of anti-INAs can be generally correlated with thermal hysteresis activity.

In this study, the effects of different anti-INAs on heterogeneous ice nucleation initiated by particles of silver iodide (AgI), which is a typical inorganic INA,<sup>38</sup> in emulsified aqueous solutions were measured. AFP I, AFP III, both of which are fish AFPs, and PVA were used as known anti-INAs, and three other synthetic polymers not currently considered anti-INAs (i.e., poly(vinylpyrrolidone) (PVP), poly(ethylene glycol) (PEG), and polyacrylamide (PAM)) were also used for comparison. On the basis of the experimental results, we discussed how completely each anti-INA and non-anti-INA could inhibit the ice nucleating activity of AgI and also discussed the correlation between anti-ice nucleating activity and thermal hysteresis activity.

## 2. EXPERIMENTAL SECTION

**2.1. Materials.** Three known anti-INAs were used here, namely, two types of AFPs, AFP I from winter flounder, *Pleuronectes americanus* (A/F Protein, type I, molecular weight  $M \approx 3300$ ) and AFP III from ocean pout, *Macrozoarces americanus* (A/F Protein, type III,  $M \approx 7000$ ), and a synthetic polymer PVA (Aldrich, weight-average molecular weight  $M_w = 13\,000\text{--}23\,000$ , degree of hydrolysis of 0.98), along with three other synthetic polymers not currently considered anti-INAs, namely, PVP (Aldrich,  $M = 10\,000$ ), PEG (Aldrich, number-average molecular weight  $M_n = 200, 1000 (950\text{--}1050), 2050 (1900\text{--}2200), 3400, and 10\,000$ ), PAM (Aldrich,  $M_w = 10\,000$ ). For PEG,  $M_n = 10\,000$  was used unless otherwise specified. All the commercial AFPs and synthetic polymers evaluated here were used without further purification. Aqueous solutions of these AFPs and synthetic polymers were prepared by using purified deionized water (Millipore, Elix-UV-3 and Academic-A10) as the solvent. AgI (Sigma-Aldrich, 99%) was used as an inorganic INA. To make water-in-oil (W/O) emulsions, *n*-heptane (Wako Pure Chemical Industries, spectrochemical analysis grade) was used as a continuous phase and sorbitan tristearate (Sigma, SPAN 65) was used as an emulsifier.

**2.2. W/O Emulsion.** W/O emulsions containing AgI particles were prepared, taking care to avoid contamination, as follows. AgI particles (0.2 g) were suspended in 4 mL of purified deionized water in a disposable glass vial. The

suspension was sonicated (Emerson Electric, Branson model 1510) in the glass vial for 60 min at room temperature and then immediately filtrated through a filter paper (Whatman, ashless grade 41) to remove relatively large AgI particles and aggregates from the suspension. Thus, only AgI particles less than 3 μm in diameter remained in the suspension.

Aqueous solutions of each AFP or synthetic polymer were prepared at three times the desired final concentration, and then 1 mL of the respective aqueous solution was mixed with 2 mL of the AgI suspension. For comparison, 1 mL of purified deionized water mixed with 2 mL of the AgI suspension was also prepared. Each mixture was then emulsified in 6 mL of *n*-heptane in a disposal glass vial, in which 4 wt % SPAN 65 had been dissolved at 80 °C, by stirring with a homogenizer (IKA, T-25, and S25N-8G) at 12 000 rpm for 6 min. The W/O emulsion was finally diluted 10-fold with *n*-heptane so that the dispersed aqueous droplets would not overlap when observed by optical microscopy. More details of the method to prepare W/O emulsion are described elsewhere.<sup>32</sup>

By using W/O emulsions, foreign particles contaminating aqueous solutions can be isolated to only a small fraction of droplets. It is already confirmed that when using W/O emulsions prepared by the above procedure, foreign particles have only negligible influence on ice nucleation.<sup>32</sup>

**2.3. Ice Nucleation Temperature.** Ice nucleation temperature of the aqueous solutions or water containing AgI particles was determined for each droplet in the W/O emulsion by observing the freezing of the droplets by using optical microscopy. Most of the experimental procedures used here have been described elsewhere,<sup>32</sup> so only a brief description and modifications are given here.

The emulsion sample was placed between two transparent cover glasses and then sealed around the edges using grease (Daikin Industries, DEMNUM L-65). The upper cover glass was 15 mm in diameter, and the lower was 18 mm. The sample thickness was controlled at about 50 μm by stainless steel spacers (1 × 1 mm). The aqueous droplets were in contact with the lower cover glass with a contact angle of about 65° and thus had a spherical cap shape. In this study, the droplet diameter  $d$  was defined as the diameter of a sphere having the same volume as the observed spherical cap, assuming a contact angle of 65°.

The emulsion film sample, with the two cover glasses, was placed in a copper sample cell and then cooled by immersing one end of the copper cell body in liquid nitrogen. The cooling rate was maintained at 4 °C min<sup>-1</sup> from 10 to -50 °C by using a foil heater attached to the copper cell. The emulsion sample temperature  $T$  was measured by a T-type sheath thermocouple (1 mm diameter), which was embedded in the copper cell body. While embedded in the copper cell body, the thermocouple was calibrated by measuring the melting temperature of ice and *n*-decane (Aldrich, anhydrous grade) in the copper cell.

The emulsion samples were observed by using transmitted light microscopy (Keyence, VB-7000, VB-7010, and VH-Z100). The light was passed through a 0.5 mm diameter aperture made in the copper cell body. Before cooling, for each droplet in the observed images at 3000× magnification,  $d$  was measured and the number of AgI particles inside the droplet ( $N_{\text{AgI}}$ ) was counted. Then, during cooling, the observed images were recorded at 2000× magnification from 0 to -45 °C at intervals of 1 s, corresponding to a temperature decrease of 0.07 °C. The ice nucleation temperature  $T_f$  was determined for each droplet

as the sample temperature at which the shape deformation of the droplet was detected in the observed images.

The aqueous droplets were polydispersed from 1.7 to 32.9  $\mu\text{m}$  (from  $2.6 \times 10^{-12}$  to  $1.8 \times 10^{-8}$  mL), and  $N_{\text{AgI}}$  was widely distributed from 0 to more than 10. In this study, only the data that satisfied  $5 < d < 25 \mu\text{m}$  (from  $6.5 \times 10^{-11}$  to  $8.2 \times 10^{-9}$  mL) and  $2 \leq N_{\text{AgI}} \leq 8$  were considered unless otherwise specified. The number of droplets observed in a single measurement was between 20 and 40. The emulsion sample was changed for every measurement, and thus in total, at least 60 droplets ( $n \geq 60$ ) in each aqueous solution were measured.

**2.4. Statistical Analysis.** A nonparametric Mann–Whitney U test was used to statistically assess differences in ice nucleation temperature between different solutions and water. These differences were regarded as significant if  $p < 0.05$ .

### 3. RESULTS

Figure 1 shows a representative observed image of water droplets containing AgI particles in a W/O emulsion at room

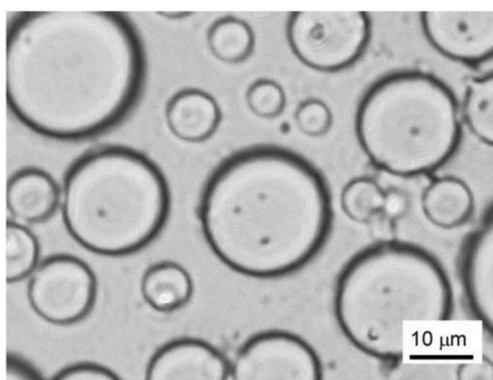
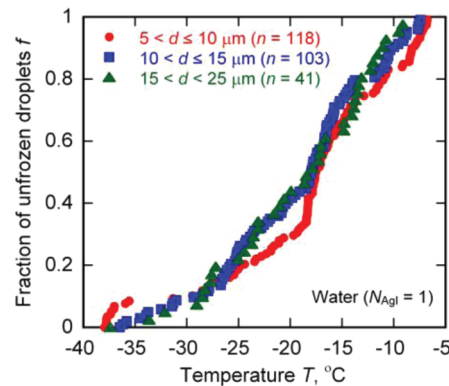


**Figure 1.** Photograph of water droplets containing AgI particles in W/O emulsion at room temperature before freezing. Movement of AgI particles inside water droplets can be seen in the video in the Supporting Information.

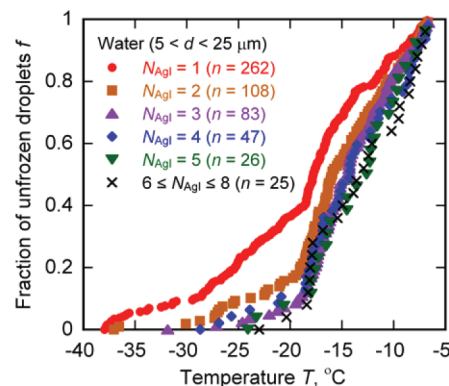
temperature. The AgI particles were distributed in both the water droplets and continuous phase. Until the droplets froze, AgI particles in the droplets of the aqueous solutions or water moved around by being repelled by each other due to their electric charge. The movement of AgI particles in the water droplets can be clearly observed in the video in the Supporting Information.

Figure 2 shows the fraction  $f$  of unfrozen droplets of water containing AgI particles as a function of  $T$  for different ranges of  $d$ . Here, only the data that satisfy  $N_{\text{AgI}} = 1$  were considered. No specific correlation between the  $f-T$  curve and  $d$  indicates that ice nucleation was initiated neither homogeneously in the interior of the droplets nor on the droplet surfaces, but heterogeneously on the surfaces of the AgI particles. All of the data that satisfied  $5 < d < 25 \mu\text{m}$  were used hereinafter because in the presence of AgI particles, the  $f-T$  curve was not influenced by  $d$ .

Figure 3 shows  $f$  for water containing AgI particles as a function of  $T$  for different  $N_{\text{AgI}}$ . Because it was difficult to accurately count  $N_{\text{AgI}}$  when  $N_{\text{AgI}} > 8$ , only the data that satisfied  $1 \leq N_{\text{AgI}} \leq 8$  were plotted. The  $f-T$  curve gradually shifted toward higher temperatures as  $N_{\text{AgI}}$  increased. However, the influence of  $N_{\text{AgI}}$  on the  $f-T$  curve was relatively small except for  $N_{\text{AgI}} = 1$ . Although, strictly speaking, droplets at constant



**Figure 2.** Fraction  $f$  of unfrozen droplets for water when  $N_{\text{AgI}} = 1$ , as a function of sample temperature  $T$ , for different ranges of droplet diameter  $d$ . Here,  $N_{\text{AgI}}$  is the number of AgI particles inside a droplet.



**Figure 3.** Fraction  $f$  of unfrozen droplets for water when droplet diameter  $d$  satisfies  $5 < d < 25 \mu\text{m}$  as a function of sample temperature  $T$  for different numbers  $N_{\text{AgI}}$  of AgI particles inside a droplet.

$N_{\text{AgI}}$  should have been considered in the data analysis, the data that satisfied  $2 \leq N_{\text{AgI}} \leq 8$  were used hereinafter because a sufficient number of data points ( $n \geq 60$ ) were required to evaluate the trend of the  $f-T$  curve.

Figure 4 shows  $f$  for water and different aqueous solutions at a concentration  $c$  of  $1.0 \times 10^{-2} \text{ mg mL}^{-1}$  (Figure 4a) and  $1.0 \text{ mg mL}^{-1}$  (Figure 4b) as a function of  $T$ . The number  $n$  of droplets analyzed for each solution is shown in Table 1. The solid line represents previously reported results for water droplets in W/O emulsions containing no INAs; the results are shown based on previous data only for the droplets that satisfied  $5 < d < 25 \mu\text{m}$ .<sup>32</sup> In this case, ice nucleation was initiated within a narrow temperature range around  $-37^\circ\text{C}$ , which coincides relatively well with the previously reported lowest  $T_f$  of various experimental data for water droplets of the same diameter range ( $5 < d < 25 \mu\text{m}$ ).<sup>1</sup> In contrast, for water droplets containing AgI particles ( $2 \leq N_{\text{AgI}} \leq 8$ ),  $T_f$  (solid circular symbol) was widely distributed between  $-37.1$  and  $-6.6^\circ\text{C}$ , and the  $f-T$  curve clearly shifted toward higher temperatures due to the high ice nucleating activity of AgI. Although the emulsifier SPAN 65 used here also induces ice nucleation in W/O emulsions in the absence of AgI,<sup>32</sup> the ice nucleating activity of SPAN 65 is negligibly low compared with that of AgI.

When the AFP or synthetic polymer solutions (except PAM) containing AgI particles were used at  $1.0 \times 10^{-2} \text{ mg mL}^{-1}$ , the  $f-T$  curves shifted toward lower temperatures compared with that of water containing AgI particles (solid circular symbols)

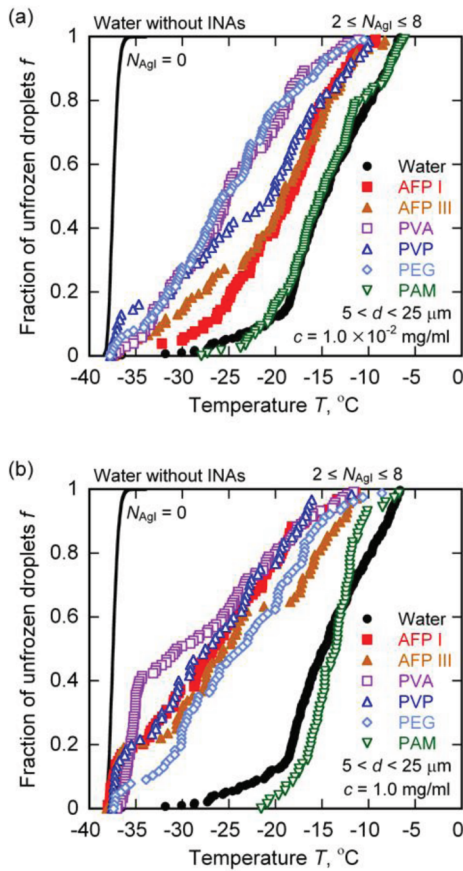


**Figure 4.** Fraction  $f$  of unfrozen droplets for water and different solutions at concentration  $c$  of (a)  $1.0 \times 10^{-2}$  mg mL<sup>-1</sup> and (b)  $1.0$  mg mL<sup>-1</sup> as a function of sample temperature  $T$ . Each droplet contained AgI particles ( $2 \leq N_{\text{AgI}} \leq 8$ ). Line represents results for water without AgI particles ( $N_{\text{AgI}} = 0$ ), rearranged from previous data.<sup>32</sup> Here,  $N_{\text{AgI}}$  is the number of AgI particles inside a droplet. For all droplets, diameter  $d$  satisfies  $5 < d < 25 \mu\text{m}$ .

(Figure 4a). PAM seemed to have no effect on the  $f-T$  curve. These results show that not only known anti-INAs (AFP I, AFP III, and PVA) but also the two other synthetic polymers (PVP and PEG) contributed to the inactivation of the ice nucleating activity of AgI even at  $c$  as low as  $1.0 \times 10^{-2}$  mg mL<sup>-1</sup>. At this  $c$ , the effectiveness of the synthetic polymers except PAM to inactivate AgI was slightly higher than that of AFPs.

When  $c$  was increased to  $1.0$  mg mL<sup>-1</sup>, the  $f-T$  curves shifted further toward lower temperatures for all the solutions except the PAM solution (Figure 4b). These results show that although PAM seemed to have no effect on the ice nucleating activity of AgI, the other synthetic polymers and AFPs effectively inactivated AgI. Especially, for the AFP I, AFP III, PVP, and PEG solutions, the  $f-T$  curves coincide well with that of water without AgI particles (solid line) in the lower temperature portion, indicating that the ice nucleating activity of AgI was completely inactivated by AFP I, AFP III, PVP, and PEG in a non-negligible fraction of the emulsified droplets. In droplets of PVA solution in W/O emulsions, PVA molecules themselves reportedly act as INAs and increase  $T_f$  even if other INAs are removed from water.<sup>32,39</sup> Because this increase in  $T_f$  caused by  $1.0$  mg mL<sup>-1</sup> PVA is about  $2$  °C,<sup>32,39</sup> the result in Figure 4b suggests complete inactivation of the ice nucleating activity of AgI also by PVA in a non-negligible fraction of the droplets.

**Table 1.** Fraction  $F$  of Droplets in Which Ice Nucleation Temperature  $T_f$  Was Identical with That of Water Containing No INAs for Different Solutions Containing AgI Particles ( $2 \leq N_{\text{AgI}} \leq 8$ ), Where  $N_{\text{AgI}}$  Is the Number of AgI Particles inside a Droplet

solution	$c$ [mg mL <sup>-1</sup> ]	$F (= n_{10}/n)^a$
AFP I (M 3300)	$1.0 \times 10^{-2}$	0.03 (3/104)
	1.0	0.16 (15/94)
AFP III (M 7000)	$1.0 \times 10^{-4}$	0.06 (4/64)
	$1.0 \times 10^{-2}$	0.03 (2/77)
PVA ( $M_w$ 13 000–23 000) <sup>b</sup>	1.0	0.16 (11/68)
	$1.0 \times 10^{-2}$	— <sup>c</sup>
PVP (M 10 000)	1.0	0.38 (45/118) <sup>d</sup>
	$1.0 \times 10^{-4}$	0.00 (0/76)
PEG ( $M_n$ 200)	$1.0 \times 10^{-3}$	0.03 (3/102)
	1.0	0.11 (7/62)
PEG ( $M_n$ 1000)	1.0	0.15 (9/60)
	$1.0 \times 10^{-2}$	0.00 (0/66)
PEG ( $M_n$ 2050)	1.0	0.03 (2/67)
	$1.0 \times 10^{-2}$	0.07 (4/60)
PEG ( $M_n$ 3400)	1.0	0.10 (11/106)
	$1.0 \times 10^{-2}$	0.06 (6/101)
PEG ( $M_n$ 10 000)	1.0	0.05 (4/77)
	$1.0 \times 10^{-2}$	0.00 (0/118)
PAM ( $M_w$ 10 000)	1.0	0.00 (0/72)
	$1.0 \times 10^{-2}$	0.00 (0/1289)
water	—	0.00 (1/289)

<sup>a</sup> $n_{10}$  is the number of droplets in which  $T_f < T_{f10}$ .  $T_{f10}$  was defined as the temperature at which 10% of water droplets containing no INAs were frozen, and  $T_{f10}$  for water containing no INAs is  $-36.8$  °C. <sup>b</sup> $T_f$  for a PVA solution containing no INAs is considerably higher than that in pure water.<sup>32,39</sup> Therefore, only for PVA solutions,  $T_{f10}$  should be defined not for water, but for PVA solutions themselves. <sup>c</sup>Because  $T_{f10}$  for a PVA solution at  $1.0 \times 10^{-2}$  mg mL<sup>-1</sup> is unknown,  $n_{10}$  could not be counted and thus  $F$  could not be evaluated. <sup>d</sup> $n_{10}$  was counted based on  $T_{f10} = -34.7$  °C in a PVA solution at  $1.0$  mg mL<sup>-1</sup>.

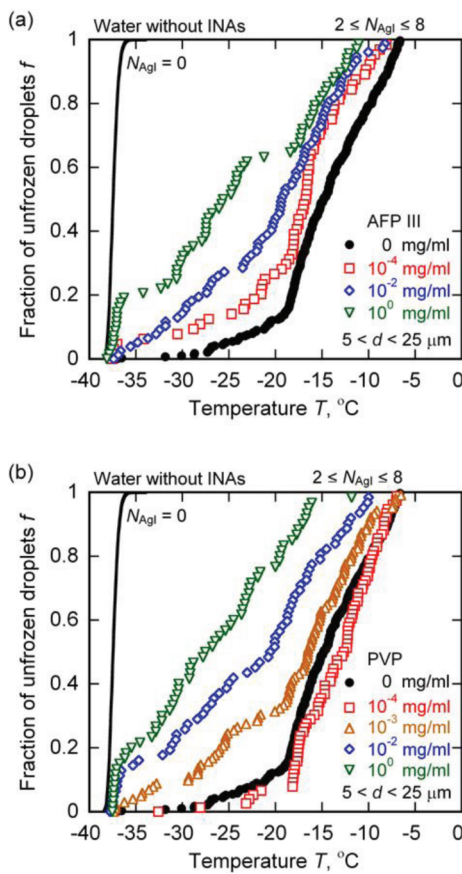
Figure 5 shows  $f-T$  curves for aqueous solutions of AFP III at different  $c = 0$  (water),  $1.0 \times 10^{-4}$ ,  $1.0 \times 10^{-2}$ , and  $1.0$  mg mL<sup>-1</sup> (Figure 5a) and PVP at different  $c = 0$  (water),  $1.0 \times 10^{-4}$ ,  $1.0 \times 10^{-3}$ ,  $1.0 \times 10^{-2}$ , and  $1.0$  mg mL<sup>-1</sup> (Figure 5b). For both solutions, the  $f-T$  curves shifted toward higher temperatures as  $c$  was decreased. When  $c$  was decreased to  $1.0 \times 10^{-4}$ , the ice nucleating activity of AgI was no longer effectively inactivated by AFP III and PVP.

Figure 6 shows  $f-T$  curves for PEG solutions at  $1.0 \times 10^{-2}$  mg mL<sup>-1</sup> for different  $M_n = 200, 1000, 2050, 3400$ , and  $10 000$ . The  $f-T$  curves clearly shifted toward higher temperatures as  $M_n$  was decreased below 2050. When  $M_n$  was decreased to 200, the ice nucleating activity of AgI was no longer inactivated by PEG.

#### 4. DISCUSSION

The results in Figure 4 show that the ice nucleating activity of AgI was inactivated not only by AFP I, AFP III, and PVA, which are already known as anti-INAs, but also by PVP and PEG, which were not previously known to be anti-INAs, whereas PAM had no effect on ice nucleation initiated by AgI. To confirm these results, first we review a few previously proposed mechanisms of the ice nucleating activity of AgI, and then, on the basis of these mechanisms, we discuss the reproducibility of our experiments on ice nucleation initiated by AgI particles.

AgI reportedly has a crystal structure similar to that of ice Ih<sup>38,40,41</sup> and thus enhances ice nucleation by reducing the



**Figure 5.** Fraction  $f$  of unfrozen droplets for (a) AFP III and (b) PVP solutions at different concentrations as a function of sample temperature  $T$ . Each droplet contained AgI particles ( $2 \leq N_{\text{AgI}} \leq 8$ ). Line represents results for water without AgI particles ( $N_{\text{AgI}} = 0$ ), rearranged from previous data.<sup>32</sup> Here,  $N_{\text{AgI}}$  is the number of AgI particles inside a droplet. For all droplets, diameter  $d$  satisfies  $5 < d < 25 \mu\text{m}$ .

interfacial free energy.<sup>41,42</sup> This suggests that the ice nucleating activity of AgI varies with the crystallographically different

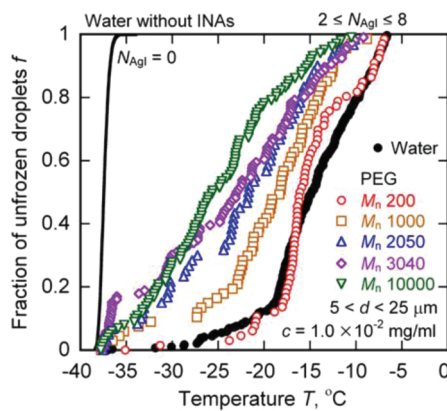


**Figure 6.** Fraction  $f$  of unfrozen droplets for PEG solutions at a concentration  $c$  of  $1.0 \times 10^{-2} \text{ mg mL}^{-1}$  for different number-average molecular weights  $M_n$ , as a function of sample temperature  $T$ . Each droplet contained AgI particles ( $2 \leq N_{\text{AgI}} \leq 8$ ). Line represents results for water without AgI particles ( $N_{\text{AgI}} = 0$ ), rearranged from previous data.<sup>32</sup> Here,  $N_{\text{AgI}}$  is the number of AgI particles inside a droplet. For all droplets, diameter  $d$  satisfies  $5 < d < 25 \mu\text{m}$ .

surfaces.<sup>40,41,43</sup> Photochemical decomposition of AgI crystals affects the ice nucleating activity,<sup>42–44</sup> probably because such decomposition changes the surface properties of AgI and thus changes the interfacial free energy.<sup>42</sup> In addition, the electric charge on AgI surfaces also affects the ice nucleating activity.<sup>45,46</sup>

In our present experiments,  $T_f$  was widely distributed for water droplets containing AgI particles, as shown by the solid circular symbols in Figure 4. If we consider the stochastic nature of heterogeneous ice nucleation, as in classical nucleation theory, such a wide range of  $T_f$  seems unlikely when assuming monodispersed AgI particles that have a uniform surface. However, if the surface properties are assumed to be nonuniform and different for each AgI particle, the wide range of  $T_f$  can be explained based on the stochastic nature of heterogeneous nucleation alone.<sup>47</sup> Therefore, the wide range of  $T_f$  in Figure 4 is probably due to the lack of reproducibility of the AgI surface properties and to the inherent nonuniform surface properties of AgI particles.

The lack of reproducibility of the AgI surface properties would most likely be due to photochemical decomposition. Although the light conditions used for observation in our current study were similar in every run, it would be difficult to reproduce the surface properties due to their sensitivity to the light conditions, such as the duration time, wavelength, and strength of the light.<sup>42–44</sup> The nonuniformity of the surface properties of AgI can be attributed to the crystallographically different surfaces of the particles. SEM images of AgI particles used in the present experiments (data not shown) revealed that the particles had random shape with no specific facets, indicating that the surface properties were not uniform.

In conclusion, the wide distribution of  $T_f$  when AgI particles are present is therefore reasonable. Considering this wide range of  $T_f$  when the number of droplets is small, the measured  $T_f$  is meaningless. However, when the number of droplets is increased, comparison of  $f-T$  curves for different conditions is meaningful.

To quantitatively compare the  $f-T$  curves, Figures 7a and 7b show the median of the ice nucleation temperature  $T_{f50}$  for different solutions at  $c = 1.0 \times 10^{-2}$  and  $1.0 \text{ mg mL}^{-1}$ , respectively.  $T_{f50}$  was defined as the temperature at which 50% of droplets were frozen. Here, the results are represented by  $-T_{f50}$ , which approximately corresponds to the degree of supercooling. At both concentrations of  $1.0 \times 10^{-2}$  and  $1.0 \text{ mg mL}^{-1}$  (Figures 7a and 7b),  $T_{f50}$  was significantly reduced by AFP I, AFP III, PVA, PVP, and PEG compared with  $T_{f50}$  for water containing AgI particles ( $2 \leq N_{\text{AgI}} \leq 8$ ) ( $p < 0.05$ , Mann–Whitney U test), whereas PAM had no significant influence on  $T_{f50}$ . These results clearly show that AFP I, AFP III, PVA, PVP, and PEG inactivate the ice nucleating activity of AgI, despite the lack of reproducibility of the AgI properties used in the present experiments.

In Figures 4–6, a portion of the  $f-T$  curves for aqueous solutions containing AgI particles at lower temperatures around  $-37^\circ\text{C}$  are similar to that of water containing no INAs. As already mentioned, such similarity suggests that AFPs and some of the synthetic polymers used in this study could completely inactivate the ice nucleating activity of AgI in a non-negligible fraction of the droplets. Here, the fraction  $F$  of droplets in which  $T_f$  was identical with that of water containing no INAs was evaluated from the data in Figures 4–6. First,  $T_{f10}$  for water containing no INAs was defined as the temperature at which 10% of the droplets were frozen. Then, if  $T_f$  in a droplet of

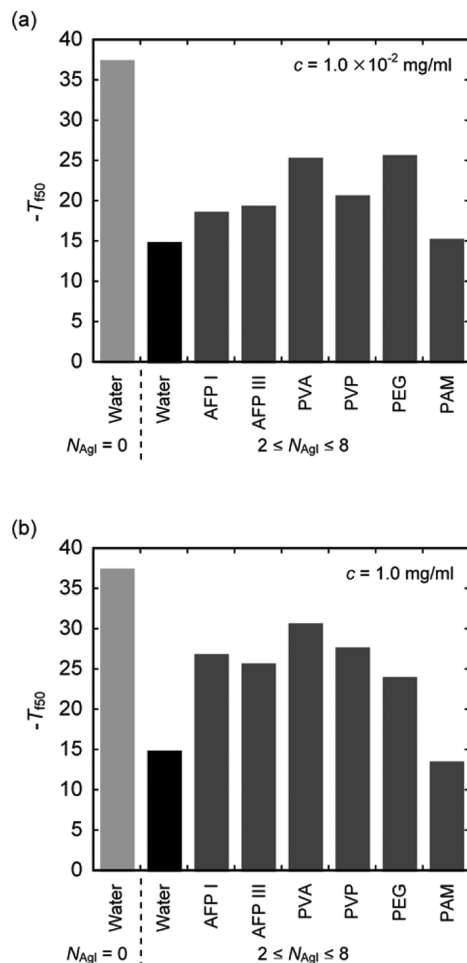


**Figure 7.** Median ice nucleation temperature  $T_{f50}$  for water and different solutions at concentration  $c$  of (a)  $1.0 \times 10^{-2} \text{ mg mL}^{-1}$  and (b)  $1.0 \text{ mg mL}^{-1}$ , when each droplet contained AgI particles ( $2 \leq N_{AgI} \leq 8$ ).  $T_{f50}$  for water without AgI particles ( $N_{AgI} = 0$ ) is also shown for reference.

aqueous solutions was lower than  $T_{f10}$ , it was considered identical with that of water containing no INAs. For each solution,  $F$  was thus evaluated.

Table 1 summarizes these results for  $F$ . It is surprising that for AFP I, AFP III, PVA, and PVP solutions at  $c = 1.0 \text{ mg mL}^{-1}$  and also for PVP and PEG ( $M_n = 3400$ ) solution at  $c = 1.0 \times 10^{-2} \text{ mg mL}^{-1}$ ,  $T_f$  in more than 10% of the droplets ( $F > 0.1$ ) was identical with that of water containing no INAs. On the contrary,  $F = 0$  for PAM solutions both at  $c = 1.0 \times 10^{-2}$  and  $1.0 \text{ mg mL}^{-1}$  as well as water containing AgI particles. Based on these results, PVP and PEG, as well as AFPs and PVA, can be categorized as anti-INAs.

The effect of melting temperature depression  $\Delta T_m$ , which is induced colligatively by the solutes, on  $T_f$  in Figures 4–6 can be explained as follows. It is known empirically that the depression of the nucleation temperature  $\Delta T_f$  of an aqueous solution increases proportionally to  $\Delta T_m$ , and thus  $T_f$  is affected by  $\Delta T_m$ .<sup>48,49</sup> However, in the present experiments,  $c$  was at most  $1.0 \text{ mg mL}^{-1}$  and the molar concentration was too low to result in measurable  $\Delta T_m$ . Therefore, the colligative effect of solutes on  $\Delta T_f$  or the  $f-T$  curves in Figures 4–6 can be neglected.

For the mechanism by which anti-INAs inhibit ice nucleation, we previously suggested that anti-INA molecules do not directly affect ice-like water clusters formed on INA

surfaces during the nucleation process.<sup>32</sup> In addition, the results shown in Figures 4–6 reveal that the anti-INAs used in this study affected the surfaces of AgI particles before ice nucleation. How the anti-INA molecules affect the AgI surfaces and thus inactivate the ice nucleating activity is our next subject of discussion as follows.

Adsorption of several polymers, including PVA,<sup>50,51</sup> PVP,<sup>50</sup> PEG,<sup>52</sup> and PAM,<sup>50</sup> on AgI surfaces in water has been extensively studied in terms of the stability of AgI colloids from an electrochemical viewpoint. The adsorption of these polymers on AgI surfaces is known basically as Langmuir type, and the adsorption process is so slow that it is regarded as almost irreversible.<sup>51</sup>

Let us consider, for example, the adsorption of PVA molecules on AgI surfaces. If PVA molecules completely cover the AgI surfaces in a flat configuration with a monolayer, the adsorbed amount of PVA molecules per unit surface area of AgI would be  $0.3 \text{ mg m}^{-2}$ , assuming an adsorption area of  $0.25 \text{ nm}^2$  for a segment of PVA molecules.<sup>51</sup> Using this adsorbed amount, the minimum  $c$  of PVA solution required for the complete coverage of the surface of AgI particles in the measured droplets with various  $d$  and  $N_{AgI}$  can be calculated as a range between  $6.4 \times 10^{-4}$  and  $9.7 \times 10^{-2} \text{ mg mL}^{-1}$ , with a median value of  $5.2 \times 10^{-3} \text{ mg mL}^{-1}$ .

In the present experiments, therefore, the complete coverage of AgI particles by PVA molecules at  $c = 1.0 \times 10^{-2} \text{ mg mL}^{-1}$  would be difficult in a certain fraction of the droplets. In addition, the reported measured maximum adsorbed amount is  $1.9$  and  $2.8 \text{ mg m}^{-2}$ ,<sup>50,51</sup> which is much higher than the theoretical value of  $0.3 \text{ mg m}^{-2}$  because most of the segments in the adsorbed PVA molecules have a loop configuration protruding into the water.<sup>51</sup> This higher amount suggests that complete coverage would be more difficult at  $c = 1.0 \times 10^{-2} \text{ mg mL}^{-1}$ . Furthermore, the measured maximum coverage of PVA molecules on the AgI surfaces was reported to be 0.7 at most in the first adsorbed layer,<sup>51</sup> and therefore complete coverage of AgI surfaces by PVA molecules is essentially impossible irrespective of  $c$ , and thus the uncovered part of AgI surfaces, which is in direct contact with water molecules, is susceptible to ice nucleation. Nevertheless, the ice nucleating activity of AgI was completely inactivated by PVA in a non-negligible fraction of the droplets (Table 1), suggesting that ice nucleation is initiated only on discrete separate sites on AgI surfaces and that PVA molecules are adsorbed selectively on these nucleation sites.

The adsorption characteristics of PVP and PEG molecules on AgI surfaces seem to be the same as that of PVA molecules; the measured maximum adsorbed amount per unit surface area of AgI is of the same order among PVA, PVP, and PEG (a few  $\text{mg m}^{-2}$ ), and the adsorption isotherm is of Langmuir type.<sup>50–52</sup> Therefore, PVP and PEG molecules inactivate the ice nucleating activity of AgI completely in a non-negligible fraction of the droplets (Table 1), in the same manner as PVA, by selective adsorption on the ice nucleating sites on AgI surfaces. Based on the similarity in the trends of the  $f-T$  curves for all the anti-INAs used in this study (Figure 4), AFP molecules might also inactivate the ice nucleating activity of AgI in the same manner, although the adsorption characteristics of AFP molecules on AgI surfaces are not yet determined.

The concentration dependency of the  $f-T$  curves in Figure 5 is compatible with the nucleation inhibition model mentioned above. On the contrary, the molecular weight dependency of the  $f-T$  curves at a constant  $c$  in Figure 6 requires further

explanation;  $M_n$  of PEG had relatively little effect on the  $f-T$  curves when  $M_n \geq 2050$ , whereas the  $f-T$  curves shifted toward higher temperatures as  $M_n$  was decreased below 2050. In Figure 6, however, the effect of not only  $M_n$  but also the molar concentration of PEG must be considered because the molar concentration decreases as  $M_n$  increases when the mass concentration  $c$  is constant. Therefore, the increase in  $M_n$  would have two opposite effects on the ice nucleating activity of AgI: (a) suppression of the ice nucleating activity of AgI because the interaction of a PEG molecule with AgI becomes stronger as  $M_n$  is increased and (b) promotion because the number of PEG molecules decreases as the PEG molar concentration is decreased. Because these two effects offset each other,  $M_n$  of PEG had relatively little effect on the  $f-T$  curves when  $M_n \geq 2050$  (Figure 6). When  $M_n < 2050$ , the suppression effect would be dominant, and thus the ice nucleating activity of AgI decreased with increasing  $M_n$ .

An unresolved issue is why PAM had no effect on the ice nucleating activity of AgI (Figure 4 and Table 1), although the measured maximum adsorbed amount per unit surface area of AgI was of the same order between PAM and the other polymers used here (a few mg m<sup>-2</sup>).<sup>50</sup> A plausible explanation for the inability of PAM to inactivate AgI is that PAM molecules could be adsorbed only on the specific sites of AgI surfaces that do not take part in ice nucleation. If so, the uncovered part of AgI surfaces occupied by water molecules should be susceptible to ice nucleation. However, there is still no evidence supporting this explanation.

As mentioned in the Introduction, AFPs show another antifreeze activity; they can completely inhibit ice growth in aqueous solutions at temperatures even below the equilibrium melting temperature.<sup>33–36</sup> The difference between the non-equilibrium freezing temperature at which ice crystals start to grow and the equilibrium melting temperature is called thermal hysteresis, which is often used to manifest the antifreeze activity. Although PVA also shows a small thermal hysteresis, PVP and PEG exhibit no detectable thermal hysteresis.<sup>37</sup> However, our present study confirms that not only AFPs and PVA but also PVP and PEG act as anti-INAs, and that their abilities to inactivate AgI are similar. In conclusion, the anti-ice nucleating activity is not directly correlated with the thermal hysteresis activity. This is not surprising because the anti-ice nucleating activity is caused by the interaction of macromolecules with INAs whereas the thermal hysteresis activity is caused by that with ice.

Finally, note that the synthetic polymers PVA, PVP, and PEG were similarly or more effective than biological AFPs in inactivating the ice nucleating activity of AgI, which is a typical inorganic INA (Figure 4 and Table 1). This might be due to the type of INA used in this study because AFPs essentially inactivate biological INAs, such as ice nucleating proteins, to survive low temperatures. Further experiments using biological organic INAs will help clarify why these synthetic polymers were more effective in the present study.

## 5. CONCLUSIONS

The effects of AFP I, AFP III, PVA, PVP, PEG, and PAM on the ice nucleating activity of AgI were measured by using W/O emulsions. The ice nucleating activity of AgI was effectively inactivated not only by AFP I, AFP III, and PVA, which are already known as anti-INAs, but also by PVP and PEG, which have not been considered anti-INAs, whereas the ice nucleating activity of AgI was not affected by PAM. Even in the presence

of AgI particles, a certain fraction, typically more than 10%, of emulsified droplets of these anti-INAs solutions at concentrations as low as 1.0 mg mL<sup>-1</sup> were supercooled to temperatures at which ice nucleation occurs in the absence of AgI particles, indicating that these anti-INAs could completely inactivate the AgI activity in a certain, non-negligible fraction of droplets.

Although the synthetic polymers used in this study are known to be adsorbed on AgI surfaces, complete coverage in the first adsorbed layer is difficult due to the configuration of these polymer molecules at the AgI/water interface. Nevertheless, the ice nucleating activity of AgI was inactivated completely in a non-negligible fraction of droplets by three of the synthetic polymers studied here, PVA, PVP, and PEG, but not by PAM. These results suggest that the ice nucleation sites on AgI surfaces are discrete and that the polymer molecules are adsorbed selectively on these nucleation sites. We speculate that AFP molecules inactivate AgI in the same manner. Although the adsorption characteristics of PAM molecules on AgI surfaces are similar to those of the other three polymers (PVA, PVP, and PEG), why the ice nucleating activity of AgI was not affected here by PAM remains an unresolved question.

This study showed that the effectiveness of PVP and PEG to inactivate the ice nucleating activity of AgI is similar to that of AFPs and PVA. However, PVP and PEG are known to exhibit no detectable thermal hysteresis, whereas AFPs and PVA exhibit thermal hysteresis, indicating that the anti-ice nucleating activity cannot be directly correlated with the thermal hysteresis activity.

## ■ ASSOCIATED CONTENT

### S Supporting Information

Video showing the movement of AgI particles in emulsified droplets. This material is available free of charge via the Internet at <http://pubs.acs.org>.

## ■ AUTHOR INFORMATION

### Corresponding Author

\*Phone +81-29-861-7272; Fax +81-29-851-7523; e-mail t-inada@aist.go.jp.

### Notes

The authors declare no competing financial interest.

## ■ ACKNOWLEDGMENTS

This study was supported by a Grant-in-Aid for Scientific Research (B) (No. 21360102) from the Japan Society for the Promotion of Science (JSPS). We are grateful to Prof. Seizo Fujikawa, Prof. Keita Arakawa, and Dr. Chikako Kuwabara (Hokkaido University, Japan) for helpful discussions on anti-ice nucleating agents.

## ■ REFERENCES

- (1) Pruppacher, H. R. *J. Atmos. Sci.* **1995**, *52*, 1924–1933.
- (2) Christner, B. C.; Morris, C. E.; Foreman, C. M.; Cai, R.; Sands, D. C. *Science* **2008**, *319*, 1214.
- (3) Zachariassen, K. E.; Kristiansen, E. *Cryobiology* **2000**, *41*, 257–279.
- (4) Gehrken, U. *J. Insect Physiol.* **1992**, *38*, 519–524.
- (5) Olsen, T. M.; Duman, J. G. *J. Comp. Physiol., B* **1997**, *167*, 105–113.
- (6) Olsen, T. M.; Duman, J. G. *J. Comp. Physiol., B* **1997**, *167*, 114–122.
- (7) Holt, C. B. *CryoLetters* **2003**, *24*, 323–330.

- (8) Du, N.; Liu, X. Y.; Hew, C. L. *J. Biol. Chem.* **2003**, *278*, 36000–36004.  
(9) Liu, X. Y.; Du, N. *J. Biol. Chem.* **2004**, *279*, 6124–6131.  
(10) Du, N.; Liu, X. Y.; Hew, C. L. *J. Phys. Chem. B* **2006**, *110*, 20562–20567.  
(11) Du, N.; Liu, X. Y. *Cryst. Growth Des.* **2008**, *8*, 3290–3294.  
(12) Xu, H.; Perumal, S.; Zhao, X.; Du, N.; Liu, X.-Y.; Jia, Z.; Lu, J. R. *Biophys. J.* **2008**, *94*, 4405–4413.  
(13) Wilson, P. W.; Osterday, K. E.; Heneghan, A. F.; Haymet, A. D. *J. J. Biol. Chem.* **2010**, *285*, 34741–34745.  
(14) Parody-Morreale, A.; Murphy, K. P.; DiCera, E.; Fall, R.; DeVries, A. L.; Gill, S. J. *Nature* **1988**, *333*, 782–783.  
(15) Wilson, P. W.; Leader, J. P. *Biophys. J.* **1995**, *68*, 2098–2107.  
(16) Kawahara, H.; Nagae, I.; Obata, H. *Biocontrol Sci.* **1996**, *1*, 11–17.  
(17) Kawahara, H.; Obata, H. *J. Antibact. Antifung. Agents* **1996**, *24*, 95–100.  
(18) Kawahara, H.; Masuda, K.; Obata, H. *Biosci. Biotechnol. Biochem.* **2000**, *64*, 2651–2656.  
(19) Yamashita, Y.; Kawahara, H.; Obata, H. *Biosci. Biotechnol. Biochem.* **2002**, *66*, 948–954.  
(20) Kasuga, J.; Hashidoko, Y.; Nishioka, A.; Yoshioka, M.; Arakawa, K.; Fujikawa, S. *Plant Cell Environ.* **2008**, *31*, 1335–1348.  
(21) Kasuga, J.; Fukushi, Y.; Kuwabara, C.; Wang, D.; Nishioka, A.; Fujikawa, E.; Arakawa, K.; Fujikawa, S. *Cryobiology* **2010**, *60*, 240–243.  
(22) Kuwabara, C.; Kasuga, J.; Wang, D.; Fukushi, Y.; Arakawa, K.; Koyama, T.; Inada, T.; Fujikawa, S. *Cryobiology* **2011**, *63*, 157–163.  
(23) Wowk, B.; Leitl, E.; Rasch, C. M.; Mesbah-Karimi, N.; Harris, S. B.; Fahy, G. M. *Cryobiology* **2000**, *40*, 228–236.  
(24) Wowk, B.; Fahy, G. M. *Cryobiology* **2002**, *44*, 14–23.  
(25) Wang, H.-Y.; Inada, T.; Funakoshi, K.; Lu, S.-S. *Cryobiology* **2009**, *59*, 83–89.  
(26) Kumano, H.; Hirata, T.; Kudoh, T. *Int. J. Refrig.* **2009**, *32*, 454–461.  
(27) Kumano, H.; Hirata, T.; Takeda, S.; Kudoh, T. *Int. J. Refrig.* **2011**, *34*, 1999–2006.  
(28) Caple, G.; Allegretto, E.; Culbertson, L. B.; Layton, R. G. *CryoLetters* **1983**, *4*, 51–58.  
(29) Baruch, E.; Mastai, Y. *Macromol. Rapid Commun.* **2007**, *28*, 2256–2261.  
(30) Watanabe, M.; Makino, T.; Okada, K.; Hara, M.; Watabe, S.; Arai, S. *Agric. Biol. Chem.* **1988**, *52*, 201–206.  
(31) Franks, F.; Darlington, J.; Schenz, T.; Mathias, S. F.; Slade, L.; Levine, H. *Nature* **1987**, *325*, 146–147.  
(32) Inada, T.; Koyama, T.; Goto, F.; Seto, T. *J. Phys. Chem. B* **2011**, *115*, 7914–7922.  
(33) DeVries, A. L. *Comp. Biochem. Physiol., B* **1988**, *90*, 611–621.  
(34) Yeh, Y.; Feeney, R. E. *Chem. Rev.* **1996**, *96*, 601–617.  
(35) Ewart, K. V.; Lin, Q.; Hew, C. L. *Cell. Mol. Life Sci.* **1999**, *55*, 271–283.  
(36) Jia, Z.; Davies, P. L. *Trends Biochem. Sci.* **2002**, *27*, 101–106.  
(37) Inada, T.; Lu, S.-S. *Chem. Phys. Lett.* **2004**, *394*, 361–365.  
(38) Vonnegut, B. *J. Appl. Phys.* **1947**, *18*, 593–595.  
(39) Ogawa, S.; Koga, M.; Osanai, S. *Chem. Phys. Lett.* **2009**, *480*, 86–89.  
(40) Vonnegut, B.; Chessin, H. *Science* **1971**, *174*, 945–946.  
(41) Passarelli, R. E., Jr.; Chessin, H.; Vonnegut, B. *Science* **1973**, *181*, 549–551.  
(42) Fletcher, N. H. *J. Meteorol.* **1959**, *16*, 249–255.  
(43) Rowland, S. C.; Layton, R. G.; Smith, D. R. *J. Atmos. Sci.* **1964**, *21*, 698–700.  
(44) Garvey, D. M. *J. Atmos. Sci.* **1973**, *30*, 165–167.  
(45) Edwards, G. R.; Evans, L. F.; LaMer, V. K. *J. Colloid Sci.* **1962**, *17*, 749–758.  
(46) Finnegan, W. G.; Chai, S. K. *J. Atmos. Sci.* **2003**, *60*, 1723–1731.  
(47) Niedermeier, D.; Shaw, R. A.; Hartmann, S.; Wex, H.; Clauss, T.; Voigtländer, J.; Stratmann, F. *Atmos. Chem. Phys.* **2011**, *11*, 8767–8775.  
(48) Rasmussen, D. H.; MacKenzie, A. P. In *Water Structure at the Water Polymer Interface*; Jellinek, H. H. G., Ed.; Plenum Press: New York, 1972; pp 126–146.  
(49) MacKenzie, A. P. *Philos. Trans. R. Soc. London, Ser. B* **1977**, *278*, 167–189.  
(50) Sugiura, M. *Bull. Chem. Soc. Jpn.* **1970**, *43*, 2604–2608.  
(51) Fleer, G. J.; Koopal, L. K.; Lyklema, J. *Kolloid Z. Z. Polym.* **1972**, *250*, 689–702.  
(52) Koopal, L. K.; Hlady, V.; Lyklema, J. *J. Colloid Interface Sci.* **1988**, *121*, 49–62.